Research Paper

The Variation of Precipitated Phase Investigated with the Usage of Nonlinear Ultrasonic Technique

Jun YOU$^{(1),(3),(4)}$, Yunxin WU$^{(1),(2),(3),(4)*}$, Hai GONG$^{(1),(2),(3),(4)}$

$^{(1)}$ *Research Institute of Light Alloys, Central South University*
Changsha, 410083, China; e-mail: csuyoujun@csu.edu.com

$^{(2)}$ *School of Mechanical and Electrical Engineering, Central South University*
Changsha, 410083, China

$^{(3)}$ *Nonferrous Metal Oriented Advanced Structural Material and Manufacturing Cooperative Innovation Center*
Central South University
Changsha, 410083, China

$^{(4)}$ *State Key Laboratory of High-Performance Complex Manufacturing*
Central South University, Changsha, 410083, China
*Corresponding Author e-mail: wuyunxin@csu.edu.cn

It is well known that nonlinear ultrasound is sensitive to some microstructural characteristics in material. This paper investigates the dependence of the nonlinear ultrasonic characteristic on Al-Cu precipitation in heat-treated 2219-T6 aluminum alloy specimens. The specimens were heat-treated at a constant temperature 155°C for different exposure times up to 1800 min. The nonlinearity parameter and the changes of precipitates phase were measured for each of the artificially aged specimens. The experimental results show fluctuations in the fractional change in nonlinear parameter ($\Delta\beta/\beta_0$) and the changes of precipitated phase over the aging time, but with an interesting correlation between the fractional change in nonlinear parameter ($\Delta\beta/\beta_0$) and the change of precipitate phase over the aging time. Through the experimental data results, the fractional change in nonlinear parameter ($\Delta\beta/\beta_0$) and the change of precipitate phase over the aging time were fitted curve. Microstructural observations confirmed that those fluctuations are due to the formation and evolution of precipitates that occur in a unique precipitation sequence in this alloy. These results suggest that the nonlinear ultrasonic measurement can be useful for monitoring second phase precipitation in the 2219-T6 aluminum alloy.

Keywords: nonlinear ultrasound; Al-Cu precipitation; 2219-T6 aluminum alloy; precipitates phase.

1. Introduction

The 2219 aluminum alloy has numerous advantages as compared to other aluminum alloys including medium strength, low specific strength, low cost, high formability, good weldability, and high corrosion resistance (DEMIR, GÜNDÜZ, 2009; TROEGER, STARKE, 2000; OZTURK *et al.*, 2010) and has been widely used in construction, automotive industry (e.g. wheels, panels, and vehicle structure), aircraft (e.g. fuselage skins), and marine engineering (OZTURK *et al.*, 2010). The 2219 aluminum alloy is a precipitation-hardened

alloy which mechanical properties can be manipulated by the heat treatment (EDWARDS, 1998) at room temperature (natural aging) or at a certain designated temperature. The T6 heat treatment is most common and can largely improve the mechanical properties (EDWARDS *et al.*, 1998; BUHA *et al.*, 2007; RAJASEKARAN *et al.*, 2012).

Microscopy using optical microscope (OM), scanning electron microscope (SEM) (BENAL *et al.*, 2007; SIDDIQUI *et al.*, 2000) and transmission electron microscope (TEM) (YASSAR *et al.*, 2011; MIAO, LAUGHLIN, 1999; FANG *et al.*, 2010) has been conventionally em-

ployed to evaluate heat-treatment induced microstructural changes. The microscopy is extremely powerful in general but it is a sample-based laboratory characterization method. In the meantime, there is a huge demand in different industries for nondestructive evaluation (NDE) techniques which can enable an *in situ* monitoring/evaluation of the material states of field structures. Among others, ultrasonic NDE techniques are probably most attractive.

In particular, nonlinear ultrasonic techniques have been considered as a potential NDE tool for the assessment of microstructural changes in materials. These techniques are based on the fact that nonlinear ultrasound interacts highly sensitively with material microstructures such as dislocations and precipitates. Therefore, from measured nonlinear ultrasonic characteristics it may be possible to evaluate the changes in microstructures during different thermal processes. One of the typical nonlinear ultrasonic phenomena is the second harmonic generation where a finite amplitude monochromatic ultrasonic wave propagating in the material is distorted and a second harmonic wave is generated.

In the case of thermal aging, the precipitates produce local strain fields, may also produce dislocations around them (XIANG *et al.*, 2014), and interact with dislocations (CANTRELL, YOST, 2000; METYA *et al.*, 2008), and all of these lead to changes in the ultrasonic nonlinearity parameter. There are some investigations on the precipitate dependent nonlinear ultrasonic characteristics in heat-treated alloys.

However, no accurate research has been performed on the variations of the ultrasonic nonlinearity parameter and the changes of precipitates phase and possible correlation between these parameters during artificial aging of 2219-T6 aluminum alloy. Furthermore, the morphology of the precipitates phase is closely associated with the strength of the material. If the growth rate of the precipitates phase can be detected by nonlinear ultrasound and the morphological characteristics of the precipitates phase can be predicted, it will be of great help to calculate the strength of the material, which will also greatly reduce the other workload. Most studies have been limited to the measurement of the relative parameter, which is defined by the amplitude of harmonic signals instead of those of the displacements (KIM *et al.*, 2016). However, they have not analyzed the microstructural evolution to verify the nonlinear ultrasonic results and the experimental results were limited to showing the relative change in the ultrasonic nonlinearity parameter.

In this study, we investigate the correlation between the changes of ultrasonic nonlinearity parameter and the precipitates phase varied due to the thermal aging in 2219-T6 aluminum alloy. The specific experimental procedure is shown in Fig. 1.
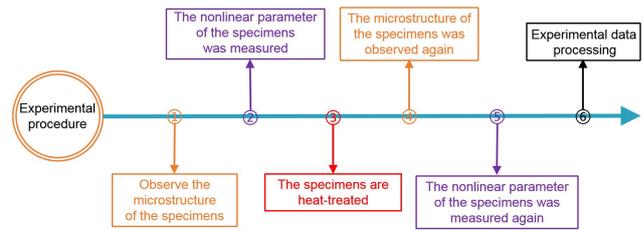

Fig. 1. Experimental procedure.

Firstly, a scanning electron microscopy (SEM) was used to observe the microstructure of the specimens and obtain the distribution of the precipitates phase. A RITEC SNAP RAM-5000 high power ultrasonic system was used for ultrasonic measurements. The accurate ultrasonic measurements were conducted using the contact piezoelectric detection method (DACE *et al.*, 1991) to determine the ultrasonic nonlinearity parameter β. After the ultrasonic measurements, heat treatment experiments were carried out to observe the changes of precipitate phase at different aging times. The heat treatment process is as follows: the 2219-T6 aluminum alloy specimens were heat-treated at a constant temperature of 155°C for different exposure times: 0, 20, 40, 60, 120, 600, and 1800 min. Next, the first and second steps of the experiment were repeated to compare the change of the nonlinear parameter and the change of the precipitate phase before and after the heat treatment. Furthermore, after experiment data processing, the relation between fractional change in nonlinear parameter and the variation of the precipitate phase was established, and the corresponding curve was fitted.

2. Theoretical consideration

A finite amplitude monochromatic ultrasonic signal is excited on one side of the material specimen and the transmitted signal is detected on the other side. The propagating ultrasonic wave gets distorted through its nonlinear interaction with nonlinearity sources in the material, which leads to the generation of second-order harmonic component in the initially monochromatic wave. Thus, detected ultrasonic signals contain not only the fundamental, i.e. the excitation frequency, but also its second harmonic frequency. The ultrasonic nonlinearity parameter, having the physical meaning of the efficiency of the second harmonic generation, is defined as follows (KIM, JHANG, 2012; BALASUBRAMANIAM *et al.*, 2011; CANTRELL, YOST, 1997; LI *et al.*, 1985; CANTRELL, ZHANG, 1998; VISWANATH *et al.*, 2011; PARK *et al.*, 2013; KIM, JHANG, 2013; REN *et al.*, 2015; YOU *et al.*, 2019): the Hooke law of linear stress-strain relationship is valid for a homogenous and isotropic medium when the applied stress amplitude is infinitesimal. However, materials in nature exhibit nonlinear stress-strain relationship and this can

be represented by first two terms of a power series expansion of strain as given by

$$\sigma = A\varepsilon + \frac{1}{2}B\varepsilon^2 + ..., \qquad (1)$$

where σ is stress, ε is displacement gradient $\partial u/\partial x$, A is the coefficient of second order term and B is the coefficient of third order term in $\partial u/\partial x$. B is a combination of second and third order elastic constants. The equation of motion of a solid element in the absence of body forces is given by Eq. (2),

$$\rho\frac{\partial^2 u}{\partial t^2} = \frac{\partial \sigma}{\partial x}, \qquad (2)$$

where is ρ the density of material, x is the propagation distance of sound wave, and u is the displacement in the x direction. Using the relationship between strain and displacement, i.e. $\varepsilon(x,t) = \partial u(x,t)/\partial x$ for a propagating one-dimensional longitudinal wave ($u = A_1 \sin\omega t$, A_1 is amplitude and ω is angular frequency) through the isotropic material and substituting the Eq. (1) in Eq. (2), one gets

$$\rho\frac{\partial^2 u}{\partial^2 t} = A\frac{\partial^2 u}{\partial x^2} + B\frac{\partial u}{\partial x}\frac{\partial^2 u}{\partial x^2}. \qquad (3)$$

A perturbation solution is assumed to solve Eq. (3) and the solution after two iterations is given by

$$u(x,t) = A_1 \sin(kx - \omega t)$$
$$+ \frac{1}{8}\frac{B}{A}A_1^2 k^2 x \cos(2kx - 2\omega t) + ..., \qquad (4)$$

where k is the wave number. From Eq. (4), the expression for the second harmonic amplitude A_2 can be expressed as

$$A_2 = \frac{1}{8}\left(\frac{B}{A}\right)k^2 A_1^2 x. \qquad (5)$$

In Eq. (5), B/A term represents the nonlinear parameter β and upon rearranging this can be expressed as

$$\beta = \frac{8A_2}{k^2 x A_1^2}, \qquad (6)$$

where β is the second harmonic based nonlinear parameter, A_1 and A_2 are the fundamental and second-order harmonic particle displacement amplitudes and x is the propagation distance (specimen thickness). k is the wave number.

However, the nonlinear parameters β are not significantly related to the changes of precipitate phase. Formula (1) expresses the relationship between nonlinear parameters and the first and second harmonics, the correlation between precipitation phase and nonlinear parameters is not obtained from formula (1). Granato and Lüke (1956), Hikata *et al.* (1965), and Cantrell and Yost (2000) have conducted a very

detailed research on the nonlinear ultrasound. According to their research, the corresponding nonlinear parameter variation of medium can be expressed as:

$$\frac{\Delta\beta}{\beta_0} = \frac{1536\Omega R^3 \Lambda L^4 C_{11}^2 |\delta|\, r_1^3 \sqrt{n}}{5\pi\beta_0\mu^2 b^2 d^3}, \qquad (7)$$

$\Delta\beta = (\beta - \beta_0)$ is the change in the nonlinearity parameter, β_0 is the initial value of nonlinearity parameter, Ω is the conversion factor from the shear strain to longitudinal strain, R is the Schmid factor, Λ is the dislocation density, L is the pinned dislocation segment length, C_{11} is the second order elastic coefficient of isotropic materials, r_1 is the radius of precipitate, δ is the precipitate-matrix lattice misfit parameter, μ is the shear modulus of the material, and b is the Burgers vector. On the dislocation line of the whole L length, there are $n \approx L/d$ precipitated weak obstacles, and d is the distance between each precipitated phase

$$f_n = \frac{4\pi r_{\text{crit}}^3}{3d^3}, \qquad (8)$$

where f_n is the volume fraction of the precipitated phase, r_{crit} is the radius of critical nucleus of the precipitate.

According to the formulas (2) and (3), the following equation can be obtained:

$$\frac{\Delta\beta}{\beta_0} = \left(\frac{230.4\Omega R^3 \Lambda L^4 C_{11}^2 |\delta|\, r_1^3 \sqrt{n}}{\pi^2 \beta_0 \mu^2 b^2 r_{\text{crit}}^3}\right) f_n. \qquad (9)$$

Further quantitative analysis requires determination of L, n, and d. Present alloy system contains mixture of coherent and semicoherent precipitates, and the determination of these parameters is difficult as it requires an estimation of distribution function for specific type of precipitate in the mixture. After the determination the relation between $\Delta\beta/\beta_0$ and f_n, and obtaining the change of volume fraction of precipitated phase f_n, the change of precipitated phase of material after heat treatment can be effectively measured.

3. Experimental procedure

3.1. Material and heat treatments

Seven 2219-T6 aluminium alloy specimens with dimensions $40 \times 20 \times 20$ mm were prepared by cutting from an aluminum plate. Prior to testing, eight hundred mesh and one thousand object sandpaper were used to grind the surface of all the specimens. Figure 2 shows the heat treatment procedure.

3.2. Nonlinear ultrasonic measurement

A RITEC SNAP RAM-5000 high power ultrasonic system was used for ultrasonic measurements. A computer controlled transmitter-receiver capable of generating sinusoidal waveform in the tone burst mode with
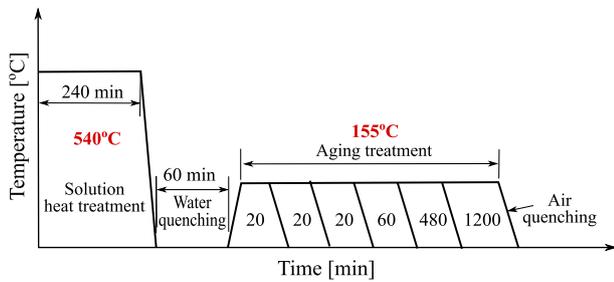
Fig. 2. Aging process diagram.

selectable number of cycles was used to drive the transducer. The RITEC system is fully computer controlled and contains two gated amplifiers of different frequency ranges, a superheterodyne receiver having capabilities of filtering, reversing phase and frequency sweeping of fundamental, second and third harmonics. The system incorporates an RF gated amplifier module to deliver very high power RF tone bursts that are needed for extracting higher harmonics and also capable of generating long bursts with numerous cycles for materials with high attenuation characteristics (MONDAL *et al.*, 2010). The experimental setup is shown in Fig. 3.
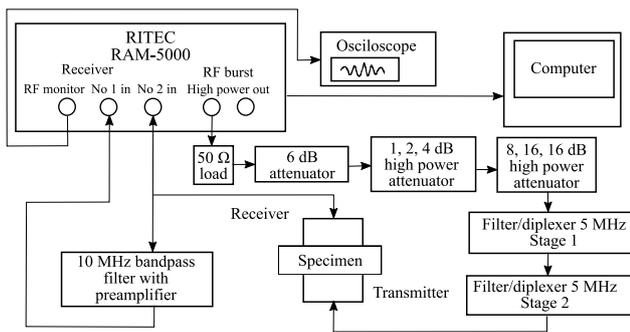

Fig. 3. Block diagram of experimental set up for measuring the nonlinear ultrasonic parameter.

4. Results and discussion

The changes in precipitated phase induced by solution aging heat treatment were evaluated by scanning electron microscopy (SEM). As shown in Fig. 4, we can observe the distribution of micro-structure in each specimen. From the percentage of the second phase in
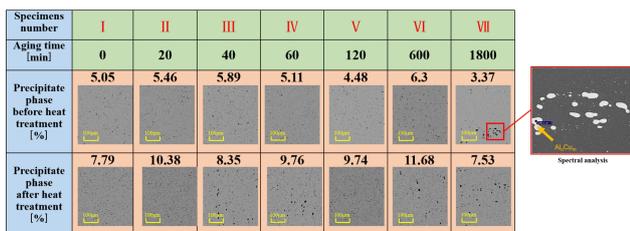

Fig. 4. Scanning electron micrographs showing fraction and distribution of precipitate phases.

the SEM figure, the change of the second phase in each specimen before and after heat treatment is seen. Before the heat treatment, the proportion of precipitated phase of each specimen was almost the same. After the heat treatment, the precipitated phase of each specimen increased significantly. A spectral analysis diagram shows the components of the precipitated phase in the SEM, and it can be seen that the precipitated phase is aluminum-copper phase.

In order to track the fractional change in the nonlinear parameter in the heat treatment, nonlinear ultrasonic measurements were carried out in the same point of each specimen and an attempt was made to correlate changes in the microstructural parameters causing such variations. Based on the experimental data, the relationship between the change in the variation of the fractional change in nonlinear parameter and the relative variation of the microstructure is obtained. Figure 5 shows the variation of the fractional change in nonlinear parameter and the relative variation of the microstructure during the heat treatment process.
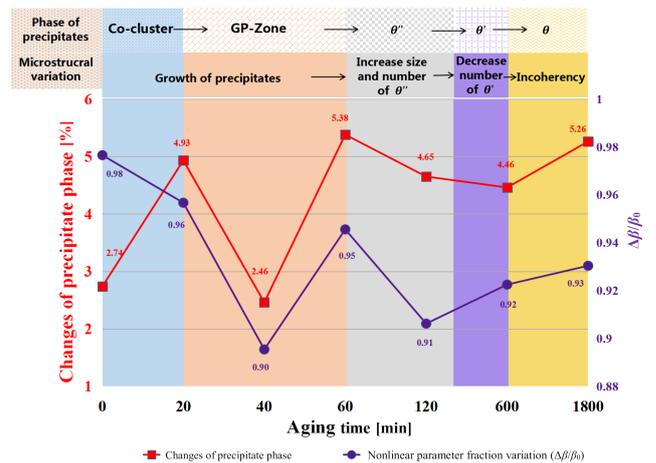

Fig. 5. Experimental results of $\Delta\beta/\beta_0$ and the relative variation of the microstructure as a function of aging time.

As shown in Fig. 5, the marked points are measured data, the measured data are connected to show the trend of the variation of the fractional change in nonlinear parameter ($\Delta\beta/\beta_0$) and the relative variation of the microstructure as a function of aging time. The variation of the fractional change in nonlinear parameter ($\Delta\beta/\beta_0$) decreases slightly and the precipitated phase increases during the first 20 min. In the following aging time, both $\Delta\beta/\beta_0$ and the precipitated phase have the same changes. They all hit the minimum at 40 minutes, and then increase. At around 60 min, $\Delta\beta/\beta_0$ and the precipitated phase reaches a positive peak. For the rest of the aging time, they slowly descended and then rose. Overall, the fractional change in nonlinear parameter ($\Delta\beta/\beta_0$) and the precipitated phase showed a good correlation over

the aging time. The variations are due to the nucleation and growth of the precipitates, which can be well described by the precipitation sequence (Demir, Gündüz, 2009; Troeger, Starke, 2000; Ozturk *et al.*, 2010; Mrówka-Nowotnik, 2010; Edwards, 1998; Buha *et al.*, 2007; Rajasekaran *et al.*, 2012).

5. Conclusion

The dependence of the nonlinear ultrasonic characteristic on the second phase precipitation in the heat-treated 2219-T6 aluminum alloy was investigated for varying thermal aging time. The 2219-T6 aluminum alloy specimens were heat-treated at a constant temperature of 155°C for aging times, 0, 20, 40, 60, 120, 600, and 1800 min. The ultrasonic nonlinearity parameter of each specimen was measured and compared with the precipitate phase obtained from SEM, and fit the relationship of them. The expression of the fitting curve is $Y = -1531 + 3270^*X + (-1739)^*X^2$. The experimental results show the variation of the fractional change in nonlinear parameter $(\Delta\beta/\beta_0)$ and the relative variation of the microstructure show an interesting correlation. The variations were explained by the precipitation sequence in the 2219-T6 aluminum alloy. According to the correlation obtained by fitting, the precipitation phase of 2219-T6 aluminum alloy can be accurately calculated by monitoring the variation of the nonlinearity parameter. This is a great help to judge the state of the material. Moreover, the nonlinearity parameter is also useful for evaluating the change of the elastic properties caused by thermal degradation and fatigue damage in industrial application.

Acknowledgment

References

1. Balasubramaniam K., Valluri J.S., Prakash R.V. (2011), Creep damage characterization using a low amplitude nonlinear ultrasonic technique, *Materials Characterization*, **62**(3): 275–286, doi: 10.1016/j.matchar. 2010.11.007.

2. Benal M.M., Shivanand H.K. (2007), Effects of reinforcements content and ageing durations on wear characteristics of Al (6061) based hybrid composites, *Wear*, **262**(5–6): 759–763, doi: 10.1016/j.wear. 2006.08.022.

3. Buha J., C R.N., Crosky A.G., Hono K. (2007), Secondary precipitation in an Al-Mg-Si-Cu alloy, *Acta Materialia*, **55**(9): 3015–3024, doi: 10.1016/j.actamat. 2007.01.006.

4. Cantrell J.H., Yost W.T. (1997), Effect of precipitate coherency strains on acoustic harmonic generation, *Journal of Applied Physics*, **81**(7): 2957–2962, doi: 10.1063/1.364327.

5. Cantrell J.H., Yost W.T. (2000), Determination of precipitate nucleation and growth rates from ultrasonic harmonic generation, *Applied Physics Letters*, **77**(13): 1952–1954, doi: 10.1063/1.1311951.

6. Cantrell J.H., Zhang X.G. (1998), Nonlinear acoustic response from precipitate-matrix misfit in a dislocation network, *Journal of Applied Physics*, **84**(10): 5469–5472, doi: 10.1063/1.368309.

7. Dace G.E., Thompson R.B., Brasche L.J.H., Rehbein D.K., Buck O. (1991), Nonlinear acoustics, a technique to determine microstructural changes in materials, [in:] *Review of Progress in Quantitative Nondestructive Evaluation*, Thompson D.O., Chimenti D.E. [Eds], Vol. 10B, pp. 1685–1692, Springer, Boston, MA, doi: 10.1007/978-1-4615-3742-7_71.

8. Demir H., Gündüz S. (2009), The effects of aging on machinability of 6061 aluminium alloy, *Materials & Design*, **30**(5): 1480–1483, doi: 10.1016/j.matdes. 2008.08.007.

9. Edwards G.A., Stiller K., Dunlop G.L., Couper M.J. (1998), The precipitation sequence in Al-Mg-Si alloys, *Acta Materialia*, **46**(11): 3893–3904, doi: 10.1016/ S1359-6454(98)00059-7.

10. Fang X., Song M., Li K., Du Y. (2010), Precipitation sequence of an aged Al-Mg-Si alloy, *Journal of Mining and Metallurgy B: Metallurgy*, **46**(2): 171–180, doi: 10.2298/JMMB1002171F.

11. Granato A., Lüke K. (1956), Theory of mechanical damping due to dislocations, *Journal of Applied Physics*, **27**(6): 583–593, doi: 10.1063/1.1722436.

12. Hikata A., Chick B.B., Elbaum C. (1965), Dislocation contribution to the second harmonic generation of ultrasonic waves, *Journal of Applied Physics*, **36**(1): 229–236, doi: 10.1063/1.1713881.

13. Kim C.S., Jhang K.Y. (2012), Fatigue-induced micro-damage characterization of austenitic stainless steel 316 using innovative nonlinear acoustics, *Chinese Physics Letters*, **29**(6): 060702, doi: 10.1088/0256-307x/29/6/060702.

14. Kim J., Jhang K.Y. (2013), Evaluation of ultrasonic nonlinear characteristics in heat-treated aluminum alloy (Al-Mg-Si-Cu), *Advances in Materials Science and Engineering*, **2013**: Article ID 407846, doi: 10.1155/ 2013/407846.

15. Kim J., Song D.G., Jhang K.Y. (2016), Absolute measurement and relative measurement of ultrasonic nonlinear parameters, *Research in Nondestructive Evaluation*, **28**(4): 211–225 doi: 10.1080/09349847. 2016.1174322.

16. Li P., Yost W.T., Cantrell J.H., Salama K. (1985), Dependence of acoustic nonlinearity parameter on second phase precipitates of aluminum alloys,

IEEE 1985 Ultrasonics Symposium, pp. 1113–1115, doi: 10.1109/ULTS-YM.1985.198690.

17. Metya A., Ghosh M., Parida N., Sagar S.P. (2008), Higher harmonic analysis of ultrasonic signal for ageing behaviour study of C-250 grade maraging steel, *NDT & E International*, **41**(6): 484–489, doi: 10.1016/j.ndteint.2008.01.008.

18. Miao W.F., Laughlin D.E. (1999), Precipitation hardening in aluminum alloy 6022, *Scripta Materialia*, **40**(7): 873–878, doi: 10.1016/S1359-6462(99)00046-9.

19. Mondal C., Mukhopadhyay A., Sarkar R. (2010), A study on precipitation characteristics induced strength variation by nonlinear ultrasonic parameter, *Journal of Applied Physics*, **108**(12): 124910, doi: 10.1063/1.3524526.

20. Ozturk F., Sisman A., Toros S., Kilic S., Picu R.C. (2010), Influence of aging treatment on mechanical properties of 6061 aluminum alloy, *Materials & Design*, **31**(2): 972–975, doi: 10.1016/j.matdes.2009.08.017.

21. Park J., Kim M., Chi B., Jang C. (2013), Correlation of metallurgical analysis & higher harmonic ultrasound response for long term isothermally aged and crept FM steel for USC TPP turbine rotors, *NDT & E International*, **54**: 159–165, doi: 10.1016/j.ndteint.2012.10.008.

22. Rajasekaran S., Udayashankar N.K., Nayak J. (2012), T4 and T6 treatment of 6061 Al-15 Vol.% SiCp composite, *ISRN Materials Science*, **2012**: 1–5, doi: 10.5402/2012/374719.

23. Ren G., Kim J., Jhang K.Y. (2015), Relationship between second- and third-order acoustic nonlinear parameters in relative measurement, *Ultrasonics*, **56**: 539–544, doi: 10.1016/j.ultras.2014.10.009.

24. Siddiqui R.A., Abdullah H.A., Al-Belushi K.R. (2000), Influence of aging parameters on the mechanical properties of 6063 aluminium alloy, *Journal of Materials Processing Technology*, **102**(1–3): 234–240, doi: 10.1016/S0924-0136(99)00476-8.

25. Troeger L.P., Starke, Jr E.A. (2000), Microstructural and mechanical characterization of a superplastic 6xxx aluminum alloy, *Materials Science and Engineering*: A, **277**(1–2): 102–113, doi: 10.1016/S0921-5093(99)00543-2.

26. Viswanath A., Rao B.P.C., Mahadevan S., Parameswaran P., Jayakumar T., Raj B. (2011), Nondestructive assessment of tensile properties of cold worked AISI type 304 stainless steel using nonlinear ultrasonic technique, *Journal of Materials Processing Technology*, **211**(3): 538–544, doi: 10.1016/j.jmatprotec.2010.11.011.

27. Xiang Y., Deng M., Xuan F.Z. (2014), Thermal degradation evaluation of HP40Nb alloy steel after long term service using a nonlinear ultrasonic technique, *Journal of Nondestructive Evaluation*, **33**: 279–287, doi: 10.1007/s10921-013-0222-8.

28. Yassar R.S., Field D.P., Weiland H. (2011), Transmission electron microscopy and differential scanning calorimetry studies on the precipitation sequence in an Al-Mg-Si alloy: AA6022, *Journal of Materials Research*, **20**(10): 2705–2711, doi: 10.1557/JMR.2005.0330.

29. You J., Wu Y.X., Gong H., Ahmad A.S, Lei Y. (2019), Determination of the influence of post – heat treatment on second-phase of Al 2219-T6 alloy using ultrasonic non-linear measurement technique, *Insight – Non-Destructive Testing and Condition Monitoring*, **61**(4): 209–213, doi: 10.1784/insi.2019.61.4.209.